



UNIVERSITY OF LEEDS

This is a repository copy of *Coverage and Rate of Low Density ABS Assisted Vertical Heterogeneous Network*.

White Rose Research Online URL for this paper:

<https://eprints.whiterose.ac.uk/189864/>

Version: Accepted Version

---

**Proceedings Paper:**

Mugala, S, Serugunda, J, Zhang, L [orcid.org/0000-0002-4535-3200](https://orcid.org/0000-0002-4535-3200) et al. (2 more authors) (2022) Coverage and Rate of Low Density ABS Assisted Vertical Heterogeneous Network. In: Proceedings of 2022 IEEE 33rd Annual International Symposium on Personal, Indoor and Mobile Radio Communications (PIMRC). 2022 IEEE 33rd Annual International Symposium on Personal, Indoor and Mobile Radio Communications (PIMRC), 12-15 Sep 2022, Kyoto, Japan. IEEE , pp. 945-950. ISBN 978-1-6654-8054-3

<https://doi.org/10.1109/PIMRC54779.2022.9977479>

---

©2022 IEEE. Personal use of this material is permitted. Permission from IEEE must be obtained for all other uses, in any current or future media, including reprinting/republishing this material for advertising or promotional purposes, creating new collective works, for resale or redistribution to servers or lists, or reuse of any copyrighted component of this work in other works.

**Reuse**

Items deposited in White Rose Research Online are protected by copyright, with all rights reserved unless indicated otherwise. They may be downloaded and/or printed for private study, or other acts as permitted by national copyright laws. The publisher or other rights holders may allow further reproduction and re-use of the full text version. This is indicated by the licence information on the White Rose Research Online record for the item.

**Takedown**

If you consider content in White Rose Research Online to be in breach of UK law, please notify us by emailing [eprints@whiterose.ac.uk](mailto:eprints@whiterose.ac.uk) including the URL of the record and the reason for the withdrawal request.



[eprints@whiterose.ac.uk](mailto:eprints@whiterose.ac.uk)  
<https://eprints.whiterose.ac.uk/>

# Coverage and Rate of Low Density ABS Assisted Vertical Heterogeneous Network

Sheila Mugala\*, Jonathan Serugunda\*, Li Zhang<sup>†</sup>, Dorothy Okello\* and Jihai Zhong<sup>†</sup>

\*Department of Electrical and Computer Engineering, Makerere University, Kampala, Uganda

Emails: {sheila.mugala, jonathan.serugunda, dorothy.okello}@mak.ac.ug

<sup>†</sup>School of Electronic and Electrical Engineering, University of Leeds, Leeds, U.K.

Emails: {L.X.Zhang, ml18j34z}@leeds.ac.uk

**Abstract**—A vertical heterogeneous network (VHetNet) is an integration of aerial base stations (ABS) into the terrestrial cellular networks. ABSs are anticipated to enhance the communications performance of the network because they are mobile and are quick to deploy suitable for on demand coverage. They promise a low-cost solution for ubiquitous connectivity especially in developing countries where telecommunications infrastructure and the power grid are limited. Accurate and tractable frameworks are required to adequately quantify the communications performance of a VHetNet. In this paper we develop an analytical framework for determining the coverage probability and average rate of a heterogeneous network with aerial, macro and small base stations. We considered a scenario with low density of ABSs suited to financially constrained countries and those with security concerns over flying machines. The results show that there is an optimum ABS altitude and density that maximize the coverage probability at a specific signal-to-interference ratio (SIR) threshold. The average rate increases with density at low SIR threshold of -10 dB while at 0 dB the optimum density decreases with altitude.

**Index Terms**—Average rate, coverage probability, heterogeneous network, Nakagami-m channel, developing countries, vertical heterogeneous network

## I. INTRODUCTION

Aerial base stations (ABSs) are unmanned aerial vehicles (UAVs) equipped with mobile phone base stations (BSs). Low altitude platform UAVs (LAPs) are deployed up to a few kilometers above the earth's surface [1], [2]. They are cost effective and can be quickly deployed making them suitable for emergency communications such as disaster recovery networks and temporary hotspots. They, however, have limited payload (weight which they can carry such as long term evolution (LTE) equipment) and battery capacity of 10 – 40 minutes [1], [2]. ABSs can provide line of sight (LoS) links which do not suffer from shadowing and thus enhance coverage.

ABSs promise a viable solution to provide connectivity for rural areas of developing countries with no grid power and other unserved areas [2], [3]. They enhance coverage of cellular networks especially on demand since they can be quickly deployed in case of emergencies such as disasters or overloaded terrestrial BSs [4]. They can also be used to extend communications infrastructure for device to device (D2D) communications [5].

## A. Related Work

Current trends in ABS research are geared towards their integration into cellular networks with a lot of work done on two-tier networks. Stochastic geometry especially the Poisson point process (PPP) method has been applied extensively in the performance analysis of traditional or terrestrial cellular networks and more recently to the vertical heterogeneous network (VHetNet) with ABSs. The coverage probability of an aerial user in a VHetNet is derived in [3] assuming 2D PPP for the macro terrestrial BSs and 2D Binomial point process (BPP) for the aerial BS. Their coverage probability varies waveringly with the aerial user height. [4] uses the Fox-H function to formulate the coverage probability, spectral efficiency and energy efficiency for an aerial-terrestrial HetNet with low and high power BSs and clustered users. They show that the decoupled uplink and downlink give better coverage and spectral efficiency than the non-decoupled access. The coverage probability of an integrated radio access technology (RAT) aerial-terrestrial network that uses mmWave and microwaves is presented in [5]. They show that both the coverage probability and rate are improved for the integrated network. [6] analyses the downlink coverage performance of a two-tier network with ABSs and ground BSs with clustered users. They show the effect of ABS density and path loss exponent on the coverage probability and area spectral efficiency for low ABS altitude of 10 and 20 m. [7] presents the downlink coverage probability of an ABS assisted disaster recovery network. [8], [9] and [10] model both LoS and non-LoS (NLoS) ABSs with Nakagami-m channel for the small scale fading. They show that there are optimum ABS altitudes and densities that maximize the coverage probability. [10] includes terrestrial BSs in addition to the ABSs. Additionally [8] uses the Faà di Bruno's formula to solve for the derivatives of the Laplace transforms. The coverage and rate of a network consisting of UAV to UAV pairs that share the uplink of cellular users is analyzed in [11] using PPP. They provide both exact and approximate analytical solutions noting that the exact solution may be difficult to solve numerically.

Most of the research on integration of ABSs into a cellular network consider one type of terrestrial BS. Our work extends this research by including ABSs in a network with both high and low power terrestrial BSs. These three BS types constitute

a critical component of future networks to enhance coverage and spectral efficiency while minimizing power consumption. We analyze the effect of ABS operating parameters such as altitude and density on the network performance. A similar scenario is presented in [4] which analyses decoupled uplink and downlink and [12] which analyses split control/data planes to minimize handover. We next present our contributions.

## B. Contributions

- 1) Formulation of a generic analytical framework for coverage performance of an interference limited VHetNet with aerial, macro and small BSs. We focus on a network with low density deployment of ABSs. This scenario is suited for developing countries which face financial constraints and countries with strict security measures regarding UAVs and other flying machines.
- 2) Analysis of both the total coverage probability and the per tier conditional coverage probabilities as ABS parameters vary. The two major parameters are altitude and density of ABSs.
- 3) Evaluation of the average rate per user for the VHetNet. We showed that there is an optimum ABS density that maximises the average rate. It varies with altitude and signal-to-interference ratio (SIR) threshold.

The rest of this paper is organized as follows. Section II presents the system model for the VHetNet. In Section III we formulate the analytical expressions for the coverage probability and average rate. Our results and discussion are in Section IV. Section V concludes the paper.

## II. SYSTEM MODEL OF VHETNET

In this paper, we analyze the downlink performance of a wireless VHetNet which consists of terrestrial BSs and aerial BSs (ABSs). The terrestrial or ground BSs are the macro BSs (MBS or  $M$ ) and small BSs (SBS or  $S$ ). ABSs or UAVs are denoted  $U$ . In this work we used the LAPs. We assume that all the BSs in the same tier transmit with the same power,  $P_i$  where  $i \in \{M, S, U\}$ , and are deployed at the same altitude,  $h_i$ . The BSs are distributed according to a two-dimensional homogeneous PPP (2D HPPP)  $\phi_i$  with intensity  $\lambda_i$ . Our user is positioned on the ground with coordinates  $(0, 0, 0)$ . The Euclidean distance between a BS and a typical user is denoted  $r$ . The ground distance is denoted  $x$  and height of the BS is  $h$ . We focus on low density of ABSs for low cost deployment especially in developing countries. Additionally our model can be applied to security conscious countries that would prefer to have a small number of UAVs on a mission. We next describe the propagation environment and interference considerations.

### A. Propagation Environment

We include both the large scale path loss and the small scale fading for the air to ground channel (A2G) and the ground to ground channel (G2G). A2G is the channel between the aerial BSs and the ground users while G2G is the channel between the terrestrial BSs and the ground users.

1) *Air to Ground Channel*: Large scale path loss model – The PPP of ABS  $\phi_U$  is decomposed into two independent PPPs for the LoS ( $\phi_L$ ) and NLoS links ( $\phi_N$ ). We predict the probability of an LoS link existing between an ABS and a ground user denoted  $P_L(x)$  using (1) [13], [14]. It is derived from the ITU defined probability of the LoS between a terrestrial transmitter and user at specified elevations [13]. In (1),  $a$  and  $b$  are parameters that quantify the environment through which signals propagate ranging from suburban or rural to high rise urban. The angle  $\tan^{-1} \frac{h}{x}$  is the elevation angle in radians between the ABS height,  $h$ , and the Euclidean distance,  $x$ , on the ground between the projection of the ABS and a ground user.

$$P_L(x) = \frac{1}{1 + a \exp(-b(\frac{180}{\pi} \tan^{-1} \frac{h}{x} - a))} \quad (1)$$

The probability of NLoS is the complement of  $P_L(x)$  i.e.  $P_N(x) = 1 - P_L(x)$ . The PPPs of LoS ( $\phi_L$ ) and NLoS ( $\phi_N$ ) ABSs are inhomogeneous because they depend on  $x$ . Specifically, the densities of the LoS ABS  $\lambda_L = \lambda_U P_L(x)$  and of the NLoS ABS is  $\lambda_N = \lambda_U P_N(x)$ . The path loss,  $L_j$ , where  $j \in \{L, N\}$ , for LoS and NLoS respectively is given in (2) [7]. The parameter,  $\varepsilon_j$ , is the mean excess path loss over the free space path loss which accounts for the shadowing and scattering of signals by man-made structures [13]. The path loss exponents,  $\alpha_j$ , for the LoS and NLoS links differ because there is more obstruction for the NLoS.

$$L_j = \varepsilon_j (x^2 + h^2)^{-\frac{\alpha_j}{2}} \quad (2)$$

The average path loss for an A2G link is  $L_U = P_L(x) \times L_L + P_N(x) \times L_N$ .

Small scale fading model – We use the Nakagami- $m$  channel with shape parameter,  $m_j$  and scale parameter  $\Omega_j = \frac{1}{m_j}$  [5], [9]. Therefore the channel gain,  $g_j$ , between a user and ABS at  $r_j$  is modelled using the Gamma distribution  $\mathcal{G}(m_j, \frac{1}{m_j})$  whose probability density function (PDF) is given in (3).

$$f_{g_j, r_j} = \frac{m_j^{m_j} y^{m_j-1} \exp(-y m_j)}{\Gamma(m_j)} \quad (3)$$

The Gamma function in (3) is defined as:  $\Gamma(m_j) = \int_0^\infty t^{m_j-1} \exp(-t) dt$ .

2) *Ground to Ground channel (G2G)*: Large scale path loss model – We used the well-known power law path loss model in (4) with path loss exponent  $\alpha > 2$  and excess path loss  $\varepsilon_i$  for  $i \in \{M, S\}$  for MBS and SBS respectively.

$$L_i = \varepsilon_i (x^2 + h^2)^{-\frac{\alpha_i}{2}} \quad (4)$$

Small scale fading model - We assumed the Rayleigh fading channel. The Rayleigh fading power gain follows an exponential distribution with mean of unity (1) such that  $g \sim \exp(1)$ .

### B. Interference Considerations

We assume a universal frequency reuse i.e. all BSs transmit at the same frequency and are therefore potential interferers to the serving BS. Noise,  $W_0$ , is considered negligible.

### III. COVERAGE PROBABILITY AND AVERAGE RATE

#### A. Distance Distributions, Association Probabilities and Coverage Probabilities

In this section, we present the association probabilities and distance distributions that we use to obtain the coverage probability. For the rest of this section we use  $i \in \{M, S\}$  for the MBS and SBS and  $j \in \{L, N\}$  for LoS and NLoS ABS respectively. Also  $i^*$  and  $j^*$  are the complements of  $i$  and  $j$ . For instance if  $i = M$  then  $i^* = S$  and the converse is true.

**Association Probabilities** - We assume that a user is associated with a BS with the strongest received power (i.e.  $P_i G_i L_i$ ).  $G_i$  is the BS associated channel gain. We use the strongest received power because the closest BS may not necessarily provide the strongest signal due to differences in path loss especially for the NLoS ABS. We give the distance distributions in Lemma 1, closest interferer distances for each tier in Lemma 2 and association probabilities in Lemma 3.

*Lemma 1:* The PDFs of the distance between a typical user and the closest MBS, SBS, LoS ABS and NLoS ABS denoted  $f_M(x)$ ,  $f_S(x)$ ,  $f_L(x)$  and  $f_N(x)$  respectively for  $x \geq 0$  are given in (5) for  $i \in \{M, S\}$  and (6) for  $j \in \{L, N\}$ .  $P_j(x) \in \{P_L(x), P_N(x)\}$ .

$$f_i(x) = 2\pi x \lambda_i \exp(-\pi \lambda_i x^2) \quad (5)$$

$$f_j(x) = 2\pi x \lambda_U P_j(x) \exp(-2\pi \lambda_U \int_0^x z P_j(z) dz) \quad (6)$$

*Proof:* The complementary cumulative distribution function (CCDF) is the null probability of the PPP  $\exp(-\pi \lambda x^2)$ . (5) and (6) are obtained by differentiating  $(1 - CCDF)$ .

*Lemma 2:* The closest distance of interferers in tier  $j$  given that a BS in tier  $k$  provides the strongest SIR is denoted  $d_{kj}$  where  $\{k, j\} \in \{M, S, L, N\}$ .

$$d_{kj} = \max\left(\left(\frac{P_j \varepsilon_j}{P_k \varepsilon_k}\right)^{1/\alpha_j} d_k^{\alpha_k/\alpha_j}, h_j\right) \quad (7)$$

*Proof:* For the association criterion in (8) we write  $d_j$  in terms of  $d_k$  in order to obtain  $d_{kj}$ . The variable  $d = \sqrt{x^2 + h^2}$ .

$$[P_k \varepsilon_k d_k^{-\alpha_k} > \max_{j \neq k} P_j \varepsilon_j d_j^{-\alpha_j}] \quad (8)$$

In (7) the maximum criterion ensures that the closest distance of an interferer cannot be less than its deployment height for the system model in II.

*Lemma 3:* The association probabilities for the MBS,  $A_M$  and SBS,  $A_S$  are given by (9) and for the LoS,  $A_L$  and NLoS ABS,  $A_N$  are given by (10).

$$A_i = \int_0^\infty \exp(-2\pi \lambda_U \int_0^{\sqrt{d_{i1}^2 - h_u^2}} z P_L(z) dz) - (2\pi \lambda_U \int_0^{\sqrt{d_{in}^2 - h_u^2}} z P_N(z) dz) - \pi \lambda_{i^*} d_{i1}^2 f_i(r) dr \quad (9)$$

$$A_j = \int_0^\infty \exp(-2\pi \lambda_U \int_0^{\sqrt{d_{jj^*}^2 - h_u^2}} z P_{j^*}(z) dz) - \pi \lambda_M d_{jm}^2 - \pi \lambda_S d_{js}^2 f_j(r) dr \quad (10)$$

*Proof:* In (11)  $\mathbb{P}[\cdot]$  is the probability of and  $\mathbb{E}_d[\cdot]$  is the expectation with respect to  $d$ .

$$A_k = \mathbb{E}_d \left[ \prod_{j=1, j \neq k}^{j=4} \mathbb{P}[d_j > (P_j \varepsilon_j / (P_k \varepsilon_k))^{1/\alpha_j} d_k^{\alpha_k/\alpha_j}] \right] \quad (11)$$

$$= \mathbb{E}_d \left[ \prod_{j=1, j \neq k}^{j=4} \exp(-\pi \lambda_j (P_j \varepsilon_j / (P_k \varepsilon_k))^{2/\alpha_j} d_k^{2\alpha_k/\alpha_j}) \right] \quad (12)$$

We take the expectation of the probability of the expression in (8) which gives (11). Using the null probability of a PPP given that no BS is closer than distance  $(P_j \varepsilon_j / (P_k \varepsilon_k))^{2/\alpha_j} d_k^{2\alpha_k/\alpha_j}$  we obtain (12) and given the closest interferer distances in (7) we obtain (9) and (10).

The PDFs for the distances between the serving BSs and a user are given in Lemma 4.

*Lemma 4:* The PDFs for the distances between the serving BSs and a user for the MBS and SBS denoted  $f_{R_M}(x)$  and  $f_{R_S}(x)$  respectively are given by (13) and for the LoS and NLoS ABS denoted  $f_{R_L}(x)$  and  $f_{R_N}(x)$  respectively are given by (14).

$$f_{R_i}(x) = \frac{1}{A_i} \exp(-2\pi \lambda_U \int_0^{\sqrt{d_{i1}^2 - h_u^2}} z P_L(z) dz) - (2\pi \lambda_U \int_0^{\sqrt{d_{in}^2 - h_u^2}} z P_N(z) dz) - \pi \lambda_{i^*} d_{i1}^2 f_i(x) \quad (13)$$

$$f_{R_j}(x) = \frac{1}{A_j} \exp(-2\pi \lambda_U \int_0^{\sqrt{d_{jj^*}^2 - h_u^2}} z P_{j^*}(z) dz) - \pi \lambda_M d_{jm}^2 - \pi \lambda_S d_{js}^2 f_j(x) \quad (14)$$

*Proof:* We define  $\overline{F_{X_k}(x)}$  as the CCDF of distance  $x_k$  for serving BS in tier  $k$ .

$$\overline{F_{X_k}(x)} = \mathbb{P}[x_k > x | n = k] = \frac{\mathbb{P}[x_k > x] \cdot \mathbb{P}[n = k]}{\mathbb{P}[n = k]} \quad (15)$$

In (15)  $A_k = \mathbb{P}[n = k]$  given in (9) and (10). The numerator of (15) is evaluated as  $\mathbb{P}[x_k > x] \cdot \mathbb{P}[n = k] = \int_{x_{\min}}^\infty \mathbb{P}[n = k] f_K(x) dx$ . Differentiating  $1 - \overline{F_{X_k}(x)}$  with respect to  $x$  gives (13) and (14).

**Coverage Probability** - This is the probability that a user achieves an SIR larger than a pre-defined threshold,  $T$ . In this section we present the downlink total coverage probability of the VHetNet which is denoted  $P_c$  in (16). It is obtained as the weighted sum of the conditional coverage probability  $P_{ck}$  for tier  $k$  in (17).

$$P_c = \sum_k P_{ck} A_k \quad (16)$$

$$P_{ck} = \mathbb{E}_x[\mathbb{P}[SIR_k(x)] \geq T] \quad (17)$$

We define  $SIR_k(x)$  in (17) as the received SIR at a user from a BS in tier  $k$ . It is given in (18) with  $g_k$  representing

the channel gain and  $I_j$  given in (19) is the interference from tier  $j$ .

$$SIR_k(x) = \frac{P_k g_k L_k}{\sum_{j=1}^4 I_j} \quad (18)$$

$$I_j = \sum_{i \in \phi_j \setminus B_{k0}} P_j L_j h_j \quad (19)$$

Note that expression  $i \in \phi_j \setminus B_{k0}$  in (19) excludes the serving BS,  $B_{k0}$  from the PPP of BSs  $\phi_j$ .

### B. Conditional Coverage Probabilities for MBS and SBS

We derive the conditional coverage probability given that a user is served by an MBS,  $P_{cm}$  or SBS,  $P_{cs}$ . We obtain (20) from (17) by expressing the aggregate interference in (19) as the sum of the interference from the MBS ( $I_M$ ), SBS ( $I_S$ ), LoS ABS ( $I_L$ ) and NLoS ABS ( $I_N$ ).

$$\begin{aligned} P_{ci} &= \int_{h_i}^{\infty} \mathbb{P}[g_i \geq T(P_i \varepsilon_i)^{-1} z^{\alpha_i} (I_i + I_{i^*} + I_L + I_N)] f_{R_i}(z) dz \\ &= \int_{h_i}^{\infty} [\exp(-T(P_i \varepsilon_i)^{-1} z^{\alpha_i} (I_i + I_{i^*} + I_L + I_N))] f_{R_i}(z) dz \end{aligned} \quad (20)$$

Noting that the channel gain,  $g_i$ , is exponentially distributed with unity mean, we obtain (21) from (20). In theorem 1 we present the MBS or SBS coverage probability.

*Theorem 1:* The conditional coverage probability of an MBS or SBS is  $P_{ci}$  given in (22).

$$P_{ci} = \int_{h_i}^{\infty} \mathcal{L}_{ii}(w_i) \mathcal{L}_{ii^*}(w_i) \mathcal{L}_{iL}(w_i) \mathcal{L}_{iN}(w_i) f_{R_i}(z) dz \quad (22)$$

In (22) the parameter  $w_i = T(P_i \varepsilon_i)^{-1} z^{\alpha_i}$ . In Lemma 5 we present the Laplace transforms,  $\mathcal{L}_{kj}(w_k)$ .

*Lemma 5:* The Laplace transform which characterises the interference when the serving BS is an MBS or SBS from MBSs and SBSs is given in (23) for the same tier and (24) for different tier. (25) gives the Laplace transforms for the LoS and NLoS ABS.

$$\mathcal{L}_{ii}(w_i) = \exp(-2\pi\lambda_i \int_0^{\infty} (1 - \frac{1}{(1 + w_i P_i \varepsilon_i (y^2 + h_i^2)^{-\alpha_i/2})} y dy) \quad (23)$$

$$\mathcal{L}_{ii^*}(w_i) = \exp(-2\pi\lambda_{i^*} \int_{\sqrt{d_{ii^*}^2 - h_i^2}}^{\infty} (1 - \frac{1}{(1 + w_i P_{i^*} \varepsilon_{i^*} (y^2 + h_i^2)^{-\alpha_{i^*}/2})} y dy) \quad (24)$$

$$\mathcal{L}_{ij}(w_i) = \exp(-2\pi\lambda_U \int_{\sqrt{d_{ij}^2 - h_u^2}}^{\infty} (1 - \frac{1}{(1 + w_i P_U \varepsilon_j (y^2 + h_u^2)^{-\alpha_j/2})} y dy) \quad (25)$$

The closest interferer distances  $d_{ii^*}$  for terrestrial BSs and  $d_{ij}$  for ABSs are obtained from (7).

*Proof:*

$$\mathcal{L}_{ii}(w_i) = \mathbb{E}_{I_i}[\exp(-w_i I_i)] \quad (26)$$

$$= \mathbb{E}_{\phi_i, G_i}[\exp(-w_i \sum_{k \in \phi_i} P_i g_i \varepsilon_i y^{-\alpha_i})] \quad (27)$$

$$= \prod_{k \in \phi_i} \mathbb{E}_{g_i}[\exp(-w_i P_i g_i \varepsilon_i y^{-\alpha_i})] \quad (28)$$

In (28) we move  $\mathbb{E}_{g_i}$  inside the product because of the independence of  $g_i$ . We then apply the Probability Generating Functional (PGFL) ( $\exp(-2\pi\lambda \int_{r_{min}}^{\infty} (1 - f(y)) y dy$ ) where  $f(y) = \mathcal{L}(\exp(-w_i P_i g_i \varepsilon_i y^{-\alpha_i}))$ ) to obtain (23). Similarly we obtain (24) and (25).

### C. Conditional Coverage Probabilities for LoS and NLoS ABS

We present the conditional coverage probabilities of LoS and NLoS ABS in Theorem 2.

*Theorem 2:* The conditional coverage probability of an LoS,  $P_{cl}$  or NLoS ABS,  $P_{cn}$  assuming a Nakagami- $m$  channel with shape parameter  $m_j$  and scale parameter  $\frac{1}{m_j}$  is given generally as  $P_{cj}$  in (29).

$$\begin{aligned} P_{cj} &= \int_{h_u}^{\infty} \sum_{k=0}^{m_j-1} \frac{(-w_j)^k}{k!} \frac{d^k}{dw_j^k} \\ &(\mathcal{L}_{jM}(w_j) \mathcal{L}_{jS}(w_j) \mathcal{L}_{jj}(w_j) \mathcal{L}_{jj^*}(w_j)) f_{R_j}(z) dz \end{aligned} \quad (29)$$

In (29) the parameter  $w_j = m_j T(P_U \varepsilon_j)^{-1} z^{\alpha_j}$ . In Lemma 6 we present the Laplace transforms in (29).

*Proof:* We use (20) and the fact that  $g_j$  follows a Gamma distribution to obtain (30) which is rewritten in (31) using the differentiation function.

$$\begin{aligned} P_{cj} &= \int_{h_u}^{\infty} \mathbb{E}_{I_j, I_{j^*}, I_M, I_S} \left\{ \sum_{k=0}^{m_j-1} \frac{(w_j (I_j + I_{j^*} + I_M + I_S))^k}{k!} \right. \\ &\times \left. \exp(-w_j (I_j + I_{j^*} + I_M + I_S)) \right\} f_{R_j}(z) dz \end{aligned} \quad (30)$$

$$\begin{aligned} &= \int_{h_u}^{\infty} \mathbb{E}_{I_j, I_{j^*}, I_M, I_S} \left\{ \sum_{k=0}^{m_j-1} \frac{(-w_j)^k}{k!} \frac{d^k}{dw_j^k} \right. \\ &\times \left. \exp(-w_j (I_j + I_{j^*} + I_M + I_S)) \right\} f_{R_j}(z) dz \end{aligned} \quad (31)$$

The expectation function in (31) is moved inside the summation. Due to the independence of the aggregate interference from the MBSs, SBSs, LoS and NLoS UAVs we use the product of the respective Laplace transforms and obtain (29).

*Lemma 6:* The Laplace transforms which characterise the interference when the serving BS is an LoS or NLoS ABS from MBSs,  $\mathcal{L}_{jM}$  and SBSs,  $\mathcal{L}_{jS}$  are given by (32) and from LoS and NLoS ABS are given in (33) and (34) for same tier and different tier respectively.

$$\begin{aligned} \mathcal{L}_{ji}(w_j) &= \exp(-2\pi\lambda_i \int_{\sqrt{d_{ji}^2 - h_i^2}}^{\infty} (1 - \frac{1}{(1 + w_j P_i \varepsilon_i (y^2 + h_i^2)^{-\alpha_i/2})} y dy) \end{aligned} \quad (32)$$

$$\mathcal{L}_{jj}(w_j) = \exp(-2\pi\lambda_U \int_0^\infty (1 - \left\{ \frac{m_j}{(m_j + w_j P_U \varepsilon_j (y^2 + h_U^2))^{-\alpha_j/2}} \right\}^{m_j} ) y P_j(y) dy) \quad (33)$$

$$\mathcal{L}_{jj^*}(w_j) = \exp(-2\pi\lambda_U \int_{\sqrt{d_{jj^*}^2 - h_U^2}}^\infty (1 - \left\{ \frac{m_{j^*}}{(m_{j^*} + w_j P_U \varepsilon_{j^*} (y^2 + h_U^2))^{-\alpha_{j^*}/2}} \right\}^{m_{j^*}} ) y P_{j^*}(y) dy) \quad (34)$$

*Proof:*

$$= \mathbb{E}_{\phi_{j^*}} \left[ \exp \left( \prod_{k \in \phi_{j^*}} \left\{ \frac{m_{j^*}}{m_{j^*} + w_j P_U \varepsilon_{j^*} y^{-\alpha_{j^*}}} \right\}^{m_{j^*}} \right) \right] \quad (35)$$

We use (28) and the fact that  $g_{j^*}$  is a Gamma function to obtain (35). Applying PGFL to (35) we obtain (34). The proof of (33) is similar to that for (34). We obtain (32) by using  $m_{j^*} = 1$  in (35) for the Rayleigh channel.

We manually solved (29) since the second order derivative is the highest. For higher order derivatives, Faà di Bruno's formula can be applied since the manual method becomes cumbersome.

#### D. Average Rate

The average rate,  $SE$ , of a typical user is the average number of bits transmitted over a given bandwidth,  $B$ . We use the Shannon capacity formula given in (36) for tier  $k$ . In theorem 3 we present the per tier average rate.

$$SE_k = \mathbb{E}_{r_k, SIR_k} [In(1 + SIR_k)] \quad (36)$$

*Theorem 3:* The average rate of a typical user for tier  $k$ ,  $SE_k$ , is given in (37). In (37),  $P_{ck}$  is the coverage probability of tier  $k$  and  $T$  is the SIR threshold.

$$SE_k = BP_{ck} \log_2(1 + T) \quad (37)$$

*Proof:*

$$SE_k = \int_0^\infty \int_{h_k}^\infty \mathbb{P}[In(1 + SIR_k) \geq \gamma] f_{R_k}(z) dz d\gamma \quad (38)$$

We obtain (38) from (36). Then using the substitution  $T = \exp^\gamma - 1$  and the definition of  $P_{ck}$  in (17) we obtain (37). Additionally we multiply by the bandwidth and divide by  $In(2)$  to obtain the average rate in Mbps.

## IV. RESULTS

TABLE I  
SIMULATION PARAMETERS

Parameter	Value
Power(dBm): $P_M, P_S, P_U$	40, 30, 30
Altitude(m): $h_M, h_S$	50, 10
Density(/km <sup>2</sup> ): $\lambda_M, \lambda_S$	4, 10
Path loss exponent: $\alpha_M, \alpha_S, \alpha_L, \alpha_N$	3, 3, 2.5, 3
Mean excess path loss: $\varepsilon_M, \varepsilon_S, \varepsilon_L, \varepsilon_N$	0.7943, 0.7943, 0.7943, 0.01

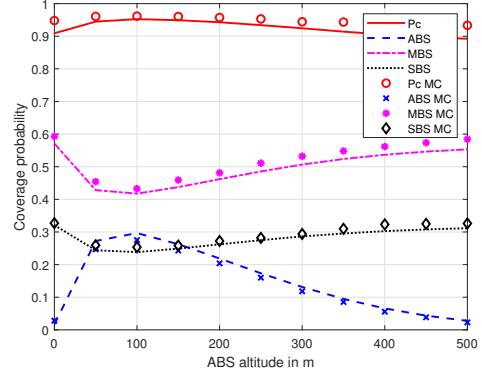


Fig. 1. Coverage probability with ABS altitude.

In this section we present our numerical results represented by lines and simulation results by markers for an area with radius of 10 km. We consider a rural environment with  $a = 4.9$  and  $b = 0.43$ . Results for the urban environment do not differ much from those presented here. Our parameters are given in Table I. The analytical results are solved using Integral a numerical integration method in MATLAB. We use Monte Carlo method (MC) to obtain the simulation results.

In Fig. 1 we present the variation of the total ( $P_c$ ) and conditional coverage probabilities of the three-tiers ( $P_{ck}$ ) with ABS/UAV altitude at SIR threshold of -15 dB and  $\lambda_U = 2 / km^2$ . The analytical results are closely matched by the Monte Carlo (MC) simulations. Both the total and ABS coverage probability initially increase and then drop. The initial increment in coverage probability is due to the increasing probability of LoS and reduction in interference from the terrestrial BSs which consequently improve the SIR from the ABSs. The coverage probability then drops due to increasing pathloss which dominates the gains from the increment in probability of LoS and reduction in interference. On the other hand the coverage probabilities of the terrestrial

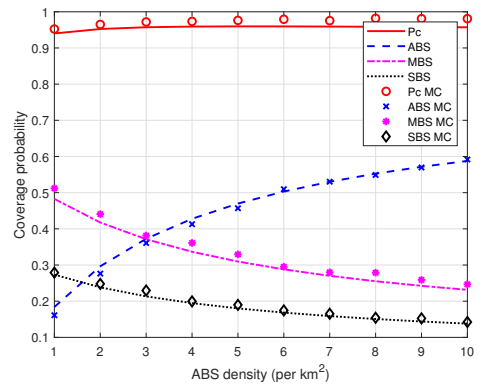


Fig. 2. Coverage probability with ABS density.

BSs (MBSs and SBSs) initially decrease as ABS altitude increases and then increase beyond the optimum ABS altitude. The strong interference from the LoS ABS links at lower

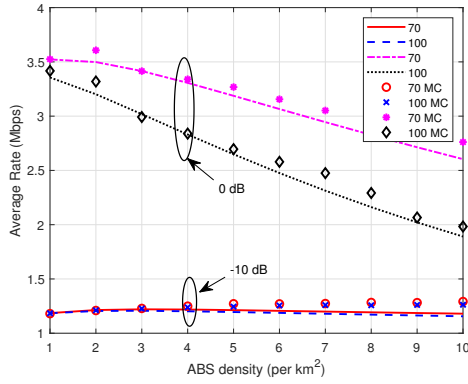


Fig. 3. Average rate with ABS density.

altitudes decreases the SIR from the MBSs and SBSs causing their coverage probabilities to reduce. For altitudes higher than the optimum the interference from the ABSs to the MBSs and SBSs reduces causing their coverage probabilities to increase.

Fig. 2 shows the effect of ABS density on the coverage probability for SIR threshold of -15 dB and ABS altitude of 100 m. We consider low ABS density i.e.  $\leq 10 / km^2$ . The results show that there is an optimum ABS density (in this case 5) at which the coverage probability is maximized. ABS coverage probability increases at the detriment of the SBS and MBS coverage probabilities because more ABSs result into a smaller coverage area for each ABS. Also MBS and SBS users with low SIR and users at the cell edges connect to ABSs. However beyond the optimum density, the coverage probability drops due to the increasing interference.

We present the variation of the average rate with ABS density for different ABS altitudes and SIR threshold values in Fig. 3. We used  $B = 10MHz$ . As a consequence of Shannon's capacity theorem, the average rate is higher at the higher SIR threshold of 0 dB. We observe that at the lower SIR threshold of -10 dB the average rate improves with ABS density for both altitudes. This increment results from an increasing coverage probability due to smaller ABS coverage area. For 0 dB and 70 m we observe that the average rate is maximized when 2 ABSs per  $km^2$  are deployed. On the contrary, at the higher altitude of 100 m increasing the number of ABSs deteriorates the coverage probability and consequently the average rate due to the growing interference.

## V. CONCLUSION

In this paper we have presented an expression for the coverage probability for an interference limited network that consists of aerial BSs and terrestrial macro and small BSs. This work considers low density deployment of ABSs suitable for financially constrained developing countries and places with extreme security concerns regarding flying machines. Both the analytical and simulated results reveal that there is an optimum ABS height and density that maximize the coverage probability at a given SIR threshold. Our results show that at a lower SIR threshold of -10 dB the average rate improves

with ABS density. However, at a higher SIR threshold of 0 dB the optimum density reduces with altitude. We recommend the analysis of clustered SBSs and ABSs for a more practical setting. Another pertinent research direction is to analyse the impact of future network technologies including coordination multi-point (CoMP) on the VHetNet performance.

## REFERENCES

- [1] S. Sekander, H. Tabassum, and E. Hossain, "Multi-tier drone architecture for 5G/B5G cellular networks: Challenges, trends, and prospects," ArXiv, 2017.
- [2] S. Mugala, D. Okello, and J. Serugunda, "Leveraging the technology of unmanned aerial vehicles for developing countries," SAIEE ARJ, vol. 111, no. 4, pp. 139–148, 2020.
- [3] N. Cherif, M. Alzenad, H. Yanikomeroglu, and A. Yongacoglu, "Downlink coverage analysis of an aerial user in vertical heterogeneous networks," in 2019 IEEE Global Communications Conference (GLOBECOM), 2019, pp. 1–6.
- [4] M. Arif, S. Wyne, K. Navaie, S. J. Nawaz, and S. H. Alvi, "Decoupled downlink and uplink access for aerial terrestrial heterogeneous cellular networks," IEEE Access, vol. 8, pp. 111172–111185, 2020.
- [5] D. Saluja, R. Singh, K. Choi, and S. Kumar, "Design and analysis of aerial-terrestrial network: A joint solution for coverage and rate," IEEE Access, vol. 9, pp. 81855–81870, 2021.
- [6] Turgut and C. Gursoy, "Downlink analysis in unmanned aerial vehicle (UAV) assisted cellular networks with clustered users," IEEE Access, vol. 6, pp. 36313 – 36324, 2018.
- [7] A. M. Hayajneh, S. A. R. Zaidi, D. C. McLernon, M. Di Renzo, and M. Ghogho, "Performance analysis of UAV enabled disaster recovery networks: A stochastic geometric framework based on cluster processes," IEEE Access, vol. 6, pp. 26215–26231, 2018.
- [8] B. Galkin, J. Kibilda, and L. A. DaSilva, "A stochastic geometry model of backhaul and user coverage in urban UAV networks," ArXiv, 2017. [Online]. Available: <https://arxiv.org/abs/1710.03701>. [Accessed: 30-May-2020].
- [9] M. Alzenad and H. Yanikomeroglu, "Coverage and rate analysis for unmanned aerial vehicle base stations with LoS/NLoS propagation," in 2018 IEEE Globecom Workshops (GC Wkshps), 2018, pp. 1–7.
- [10] C. Fan, T. Zhang, and Z. Zeng, "Coverage and rate analysis of cache-enabled vertical heterogeneous networks," IEEE Access, vol. 7, pp. 153519–153532, 2019.
- [11] M. M. Azari, G. Geraci, A. Garcia-Rodriguez, and S. Pollin, "UAV-to-UAV communications in cellular networks," IEEE Trans. Wirel. Commun., vol. 19, no. 9, pp. 6130–6144, 2020.
- [12] R. Arshad, L. Lampe, H. ElSawy, and J. Hossain, "Integrating UAVs into existing wireless networks: A stochastic geometry approach," in IEEE GC Wkshps, 2018.
- [13] A. Al-Hourani, S. Kandeepan, and A. Jamalipour, "Modeling air-to-ground path loss for low altitude platforms in urban environments," in Globecom 2014: Symposium on selected areas in communications, 2014, pp. 2898–2904.
- [14] R. Hashemi, M. R. Mili, S. Ali, H. Beyranvand, and M. Latva-Aho, "Investigating communications energy efficiency tradeoff between UAV users and small-cell users," in 2021 IEEE 32nd Annual International Symposium on Personal, Indoor and Mobile Radio Communications (PIMRC), 2021, pp. 342–347.